PERGAMON

International Journal of Heat and Mass Transfer 42 (1999) 2387–2398

International Journal of HEAT and MASS TRANSFER

Exact solution to stationary onset of convection due to surface tension variation in a multicomponent fluid layer with interfacial deformation

J.R.L. Skarda[a,*], F.E. McCaughan[b,1]

[a] *Microgravity Fluid Physics Branch, Microgravity Sciences Division, NASA Lewis Research Center, Cleveland, OH 44135, U.S.A.*

[b] *Department of Mechanical and Aerospace Engineering, Case Western Reserve University, Cleveland, OH 44135, U.S.A.*

Received 20 November 1997; in final form 3 September 1998

Abstract

Stationary onset of convection due to surface tension variation in an unbounded multicomponent fluid layer is considered. Surface deformation is included and general flux boundary conditions are imposed on the stratifying agencies (temperature/composition) disturbance equations. Exact solutions are obtained to the general N-component problem for both finite and infinitesimal wavenumbers. Long wavelength instability may coexist with a finite wavelength instability for certain sets of parameter values, often referred to as frontier points. For an impermeable/insulted upper boundary and a permeable/conductive lower boundary, frontier boundaries are computed in the space of Bond number, Bo, vs Crispation number, Cr, over the range $5\times 10^{-7} \leqslant Bo \leqslant 1$. The loci of frontier points in (Bo, Cr) space for different values of N, diffusivity ratios, and Marangoni numbers collapsed to a single curve in (Bo, $\tilde{\mathscr{D}}Cr$) space, where $\tilde{\mathscr{D}}$ is a Marangoni number weighted diffusivity ratio.

Nomenclature

Bo Bond number, $\rho g d^2/\sigma$
Cr Crispation number, $\mu\mathscr{Q}_1/\sigma d$
d thickness of layer
$\mathscr{Q}_k$ component diffusivity
$\mathscr{D}_k$ diffusivity ratio, $\mathscr{Q}_k/\mathscr{Q}_1$
$\tilde{\mathscr{D}}_k$ Ma_k weighted average of diffusivity ratios
g gravitational acceleration
h_k disturbance surface conductance
Ma_k Marangoni number, $\gamma_k\Delta\overline{S_k}d/\mu\mathscr{Q}_k$
Nu_k Nusselt number, $(h_k d/\mathscr{Q}_k)$
p pressure
Pr Prandtl number $\nu/\mathscr{Q}_1$
R correlation coefficient
s_k kth disturbance stratifying agency
S_K kth stratifying agency
u_i disturbance velocity
$\bar{u}$ basic state velocity
w normal mode velocity
x_i Cartesian coordinates.

Greek symbols
α wavenumber
γ_k kth surface tension gradient, $\partial\sigma/\partial S_k$
ζ free surface deformation
μ dynamic viscosity
ν kinematic viscosity
σ surface tension
χ normal mode stratifying agency.

Superscript
l lower boundary at $x_3 = 0$
u upper boundary at $x_3 = 1$
$-$ basic state variable.

Subscript
c critical value
fp frontier point
i, j Cartesian coordinate indices, 1, 2, 3
k associated with kth component

* Corresponding author. Tel.: 001 216 433 8728; fax: 001 216 433 8660; e-mail: skarda@lerc.nasa.gov

[1] Present address: Tribune Corporation, Chicago, IL 60611, U.S.A.

0017–9310/99/$ - see front matter
PII: S0017-9310(98)00309-3

$\sim$ dimensional variable.

1. Introduction

Multicomponent onset of convection is important in many naturally occurring phenomena and technological processes. Examples include: convection in stars, dynamics within the earth's core, oceanography, solar ponds, coating/drying processes and crystallization/solidification [1–6]. Various extensions of Rayleigh's normal mode analysis [7] to multicomponent systems have contributed to the characterization of physical conditions and fluid properties that are necessary for connective onset to occur, and the nature of the resulting instability. Double diffusive systems where convection occurs due to density variations have received the greatest attention to date [1–3, 8], although results for three or more components have also been reported [1, 4, 6].

Under certain conditions such as thin liquid films or microgravity, surface tension variations along a free surface may also induce convection. Onset of convection due to surface tension variation, also known as the Marangoni–Benard problem, was first examined by Pearson [9] with reference to drying paint films. The importance of surface deformation to the Marangoni–Benard problem was established by Scriven and Sternling [10] while gravity effects and overstability associated with a deformable free surface were investigated by Smith [11], Takashima [12, 13], and Perez-Garcia and Carneiro [14]. The Benard problem has been extensively studied and a significant portion of the immense body of literature for the single component Benard problem has been summarized by Koschmieder [15][1]. Recent reviews of thermocapillary instabilities, including the Marangoni–Benard problem are given by Davis [16] and Legros et al. [17].

In connection with microgravity materials processing applications, McTaggart [18] considered the stability of double diffusive fluid layer with a flat interface subject to surface tension variations at the free surface. In the presence of both buoyancy and surface tension variation effects, Chen and Su [19] studied the double diffusive layer where both temperature and concentration gradients are imposed across the layer. In subsequent experimental work, Tanny et al. [20] modified the linear stability analysis of Chen and Su [19] to account for a basic state with a non-linear concentration profile. The experimental and theoretical results were found to be in very good agreement [20]. Building on the work of Scriven and Sternling [10], Smith [11], and McTaggart [18], the double diffusive problem with deformation of the free surface was examined by McCaughan and Bedir [21] who neglected gravity effects. A recent numerical study by Char and Chiang [22] confirms the earlier double diffusive works [18, 19] and also examines the effects of deformation in the combined presence of gravity and surface tension forces. In Char and Chiang's investigation as well as the single component study by Perez-Garcia and Carneiro [14] a comprehensive set of stationary and oscillatory results are presented, and the existence of a single frontier point is identified. To date, only single and two component (double diffusive) systems have been considered when convective onset is due to surface tension variation.

We focus on the stationary stability behavior of a multicomponent system applying traditional methods of analysis that lead to exact solutions for a system with an arbitrary number of components, or N-components. One intrinsic value of the analytical solution is the wealth of physical insight gained from examination of the solution form and its limiting behavior. With the aid of idealized boundary conditions, exact solutions have resulted in greater physical understanding of single component and multicomponent buoyancy driven problems as well as single and double diffusive surface tension driven problems [1–11, 18, 21, 23–26]. Furthermore, analytical solutions are critical for comparison and validation of numerical computations which will ultimately be used to analyze the behavior of more complex systems [5]. In addition to further validation of published results, we find that recently reported stationary stability results for the surface tension problem can be obtained directly from our exact solutions. These solutions also permit straightforward computation of the boundary that separates the long and finite wavelength instabilities, denoted as a frontier boundary, in appropriate parameter space.

The onset of convection due to surface tension variations in a multicomponent fluid is considered in this study. Deformation of the free surface is permitted and the gravity term is also included in the normal stress condition. Mixed flux boundary conditions are applied to the stratifying agency (heat and/or composition) transport equations at both bounding surfaces. The analysis is confined to stationary onset of convection and an exact solution is derived for the problem with N-stratifying agencies. Cross-diffusive effects of interest in recent binary fluid investigations [8, 24, 26, 27] are neglected. Special cases of the solution are treated for boundary conditions typically applied in the literature [9–14, 18–22] and in the limit of infinitesimal wavenumber.

Spatial structures or normalized eigenvectors at neutral stability are briefly examined. Stationary stability in the multicomponent problem with surface deflection and gravity is explored and presented in the context of a single component system. Most significantly, frontier points and frontier boundaries, and the conditions for which they exist, are examined in parameter space for a multi-

[1] According to Koschmeider [15], more than 500 (single component) Benard related publications were written prior to 1993.

component system. Frontier boundaries are computed over the Bond number range $5\times10^{-7} \leqslant Bo \leqslant 1$, extending the previously reported range which was a single frontier point at $Bo = 0.1$ [14, 22]. Although the frontier points in (Bo, Cr) space are found to be functions of Ma_k and $\mathscr{D}_k$ in a multicomponent system, they collapse to a single frontier boundary curve in (Bo, $\tilde{\mathscr{D}}Cr$) space.

2. Mathematical formulation

We examine a fluid layer that is unbounded in its lateral dimensions, $\underset{\sim}{x}_1$, and $\underset{\sim}{x}_2$, and is of dimension $0 \leqslant \underset{\sim}{x}_3 \leqslant d$ with a deformable free surface located at $\underset{\sim}{x}_3 = d$. The velocity basic state is quiescent, $\underset{\sim}{U} = 0$. The overbar denotes a basic state variable while the underscore tilde denotes dimensional quantities. A stratified basic state is imposed on the composition and/or temperature variables that takes the form:

$$\overline{\underset{\sim}{S}_k}(\underset{\sim}{x}_3) = \overline{\underset{\sim}{S}_k}(0) - \Delta\overline{\underset{\sim}{S}}\frac{\underset{\sim}{x}_3}{\mathrm{d}}$$

where $\Delta\overline{\underset{\sim}{S}_k} = \overline{\underset{\sim}{S}_k}(0) - \overline{\underset{\sim}{S}_k}(d)$. Therefore, following [4] and [6], we denote S_k as the kth stratifying agency (composition or temperature) of a fluid layer consisting of N-stratifying agencies.

The linearized disturbance momentum and kth stratifying agency transport equation are given by eqns (1) and (2).

$$\frac{\partial \underset{\sim}{u}_i}{\partial \underset{\sim}{t}} = -\frac{1}{\rho}\frac{\partial \underset{\sim}{p}}{\partial \underset{\sim}{x}_i} + v\frac{\partial^2 \underset{\sim}{u}_i}{\partial \underset{\sim}{x}_j \partial \underset{\sim}{x}_j} \tag{1}$$

$$\frac{\partial \underset{\sim}{s}_k}{\partial \underset{\sim}{t}} = \mathscr{D}_k \frac{\partial^2 \underset{\sim}{s}_k}{\partial \underset{\sim}{x}_j \partial \underset{\sim}{x}_j} + \frac{\Delta \underset{\sim}{S}_k}{\mathrm{d}}\underset{\sim}{u}_3 \tag{2}$$

for: $i, j = 1, 2, 3$ and $k = 1, 2, \ldots, N$

The disturbance variables, u, s, and p are velocity, component and pressure, respectively, while the physical properties, density, kinematic viscosity and diffusivity are denoted as ρ, v, $\mathscr{D}_k$. The stratifying agency with the largest $\mathscr{D}$ is chosen as the $k = 1$ component. Surface tension, σ, is assumed to vary linearly with, $\underset{\sim}{S}_k$ as,

$$\sigma = \sigma_{\mathrm{ref}} + \sum_{k=1}^{N}\frac{\partial\sigma}{\partial \underset{\sim}{S}_k}(\underset{\sim}{S}_k - \underset{\sim}{S}_{\mathrm{ref}}).$$

The boundary conditions are given by eqns (3)–(8).
At $\underset{\sim}{x}_3 = 0$,

$$\underset{\sim}{u}_i = 0 \tag{3}$$

$$\left(\mathscr{D}_k \frac{\partial \underset{\sim}{s}_k}{\partial \underset{\sim}{x}_3} - \underset{\sim}{h}_k^{(l)} \underset{\sim}{s}_k\right)\Bigg|_{\underset{\sim}{x}_3 = 0} = 0 \tag{4}$$

At $\underset{\sim}{x}_3 = d$

$$\frac{\mathrm{d}\underset{\sim}{\zeta}}{\mathrm{d}\underset{\sim}{t}} = \underset{\sim}{u}_3 \tag{5}$$

$$\mu\left(\frac{\partial \underset{\sim}{u}_3}{\partial \underset{\sim}{x}_l} + \frac{\partial \underset{\sim}{u}_l}{\partial \underset{\sim}{x}_3}\right) = -\sum_{k=1}^{n}\gamma_k\left(\frac{\partial \underset{\sim}{s}_k}{\partial \underset{\sim}{x}_l} + \frac{\partial \bar{\underset{\sim}{S}}_k}{\partial \underset{\sim}{x}_3}\frac{\partial \underset{\sim}{\zeta}}{\partial \underset{\sim}{x}_l}\right) \tag{6}$$

$$-\underset{\sim}{p} + \rho g \underset{\sim}{\zeta} + 2\mu\frac{\partial \underset{\sim}{u}_3}{\partial \underset{\sim}{x}_3} = \sigma\frac{\partial^2 \underset{\sim}{\zeta}}{\partial \underset{\sim}{x}_3 \partial \underset{\sim}{x}_3} \tag{7}$$

$$\left(\mathscr{D}_k \frac{\partial \underset{\sim}{s}_k}{\partial \underset{\sim}{x}_3} + \underset{\sim}{h}_k^{(u)}\left(\underset{\sim}{s}_k + \frac{\partial \bar{\underset{\sim}{S}}_k}{\partial \underset{\sim}{x}_3}\underset{\sim}{\zeta}\right)\right)\Bigg|_{\underset{\sim}{x}_3 = \mathrm{d}} = 0 \tag{8}$$

where $l = 1, 2$ (lateral directions only) and $k = 1, 2, \ldots, N$.

A no-slip-impenetrable surface is imposed at $\underset{\sim}{x}_3 = 0$, eqn (3). Mixed disturbance flux conditions, eqns (4) and (8) are imposed at both the upper and lower boundaries on the kth stratifying agency transport equation, where $\underset{\sim}{h}_k^{(\mathrm{u})}$ and $\underset{\sim}{h}_k^{(\mathrm{l})}$ are the disturbance heat or mass transfer coefficients or surface conductances [9, 10, 18] at the upper and lower surfaces, respectively. The remaining boundary conditions at $\underset{\sim}{x}_3 = d$ are the kinematic conditions, eqn (5), tangential stress conditions, eqn (6) and normal stress condition, eqn (7).

After eliminating the perturbation pressure [9–11, 21, 23], the disturbance equations are nondimensionalized using reference values, d, $\mathscr{D}_1/d$, $d^2/\mathscr{D}_1$, $\Delta\underset{\sim}{S}_k$, $\mathscr{D}_1$ for length, velocity, time, kth component, and diffusivities, respectively. Solutions are then assumed of the form: $(u, s_k, \zeta) = (w(x_3), \chi_k(x_3), \zeta)\,\mathrm{e}^{\lambda t + i(\alpha_1 x_1 + \alpha_2 x_2)}$ with the resulting normal mode equations given by eqns (9) and (10) below, where $\alpha^2 = \alpha_1^2 + \alpha_2^2$.

$$\lambda(D^2 - \alpha^2)w = Pr(D^2 - \alpha^2)^2 w \tag{9}$$

$$\lambda\chi_k = \mathscr{D}_k(D^2 + \alpha^2)\chi_k + w \tag{10}$$

Normal mode boundary conditions are:
At $x_3 = 0$,

$$w(0) = 0 \tag{11}$$

$$Dw(0) = 0 \tag{12}$$

$$D\chi_k|_{x_3=0} - Nu_k^{(l)}\chi_k|_{x_3=0} = 0 \tag{13}$$

At $x_3 = 1$,

$$\lambda\zeta = w(1) \tag{14}$$

$$(D^2 + \alpha^2)w = -\alpha^2\sum_{k=1}^{N}\mathscr{D}_k Ma_k(\chi_k - \zeta) \tag{15}$$

$$\lambda\frac{Dw}{Pr} = (D^3 - 3\alpha^2 D)w - \frac{1}{Cr}(\alpha^4 + Bo\,\alpha^2)\zeta \tag{16}$$

$$D\chi_k|_{x_3=1} + Nu_k^{(u)}(\chi_k - \zeta)|_{x_3=1} = 0 \tag{17}$$

The surface Nusselt numbers[2] at the upper and lower boundaries, $Nu_k^{(\mathrm{u})}$ and $Nu_k^{(\mathrm{l})}$, are defined as $\underset{\sim}{h}_k^{(\mathrm{u})}\mathrm{d}/\mathscr{D}_k$ and

[2] In single component studies Nus are also denoted as surface Biot numbers, and in double diffusive analyses, often denoted as surface Nusselt and surface Sherwood numbers.

Table 1
Solution coefficients, b_{1k} and b_{2k}, for limiting disturbance flux boundary conditions

Disturbance flux boundary conditions	b_{1k}	b_{2k}
(i) $(Nu_k^{(l)}, (Nu_k^{(u)}) \to (\infty, 0)$	$\frac{1}{\alpha^2}\left(3+\frac{\operatorname{csch}\alpha\,\operatorname{sech}\alpha(\alpha\cosh\alpha-\sinh\alpha)^2}{\alpha}\right)$	$b_{2k}=0$
(ii) $(Nu_k^{(l)}, (Nu_k^{(u)}) \to (0, 0)$	$\frac{3}{\alpha^2}$	$\frac{\alpha\coth\alpha(\alpha\coth\alpha-2)+1}{\alpha^3}$

$\underline{h}_k^{(l)} d/\mathscr{D}_k$, respectively, while other dimensionless parameters are given in the Nomenclature.[3]

3. Results and discussion

3.1. Spatial shapes and normalized eigenfunctions

For stationary stability, $\lambda = 0$, thus solutions for $w(x_3)$, $\chi_k(x_3)$ and ζ, can be deduced from the above set of equations. After applying boundary conditions (11), (12) and (14) the solution for the disturbance velocity, $w(x_3)$, in terms of a single undetermined coefficient, a_1, eqn (18), is given. The solution for the kth disturbance stratifying agency, χ_k, eqn (19), contains two coefficients, b_{1k} and b_{2k}, in addition to the undetermined coefficient, a_1. The flux conditions, eqns (13) and (17), are applied to determine b_{1k} and b_{2k}, and a_1 is factored from all terms. The deformation solution, ζ, eqn (20), determined from eqn (16) also contains the undetermined coefficient, a_1.

$$w(x_3) = a_1[(1+(\alpha\coth\alpha-1)x_3)\sinh\alpha x_3 - \alpha x_3\cosh\alpha x_3] \tag{18}$$

$$\chi_k(x_3) = \frac{a_1}{4\mathscr{D}_k}\Bigg(b_{1k}\sinh\alpha x_3 + b_{2k}\cosh\alpha x_3 + \left(\frac{(\alpha\coth\alpha-1)}{\alpha^2}x_3 + (x_3)^2\right)\sinh\alpha x_3 - \frac{1}{\alpha}(3x_3 + (\alpha\coth\alpha-1)(x_3)^2)\cosh\alpha x_3\Bigg) \tag{19}$$

$$\zeta = -a_1\frac{2Cr\alpha^2\operatorname{cshc}(\alpha)}{Bo+\alpha^2} \tag{20}$$

Aside from the fact that spatial shapes, w and χ_k, need be determined as part of a parameterized stationary stability solution, they also provide physical insight to the flow behavior along the stationary stability boundary. Inspection of eqn (18) immediately reveals that a_1 affects only the magnitude of $w(x_3)$, but not its normalized eigenvector or spatial shape. The spatial shape of $w(x_3)$ is therefore invariant to all flow parameters with the exception of α, even for a multicomponent system with an arbitrary number of stratifying agencies. We observe that the stationary spatial shape of $\chi_k(x_3)$, eqn (19), is independent of all $\mathscr{D}_k$ in an N-stratifying agency system as well as independent of a_1. However, because b_{1k} and b_{2k} are, in general, functions of the α, Cr, Bo, $Nu_k^{(l)}$, and $Nu_k^{(u)}$, these parameters influence both magnitudes and spatial shapes of $\chi_k(x_3)$.

The invariance of $w(x_3)$ is meaningful in the following special but important cases, although it is less important to the general problem since the critical wavenumber is dependent on the other parameters which in turn affects the onset spatial shape. Attention is therefore focused on the important case of an impermeable (or insulated) upper surface, $Nu_k^{(u)} \to 0$, for all k, and we consider the following two limiting disturbance flux conditions at $x_3 = 0$: permeable (or conductive), $Nu_k^{(l)} \to \infty$, and impermeable (or insulated), $Nu_k^{(l)} \to 0$ for all k, $k = 1, 2, \ldots, N$. Both limits are of physical significance and reduce to the two most important single and double diffusive cases treated in the literature [9–14, 18–22].

In both limits of $Nu_k^{(l)}$, the coefficients, b_{1k} and b_{2k} are given in Table 1 and are shown to reduce to functions solely of wavenumber, α. Consequently, the stationary spatial shapes of both $w(x_3)$ and $\chi_k(x_3)$ are invariant with Ma_k, $\mathscr{D}_k$, Cr and Bo. Moreover, this property of invariance also applies to any combination of the two flux limits of a multicomponent system with N-stratifying agencies. Therefore if the spatial shapes or normalized eigenvectors are known for a given α, for example, along a stationary stability boundary in (α, Ma_k) space, for one parameter set of (Ma_l, $\mathscr{D}_l$, Cr, Bo) (for $l \neq k$) then the normalized eigenvectors are the same for any other set of (Ma_l, $\mathscr{D}_l$, Cr, Bo). As observed in Section 3.3 on frontier points, the shape of the neutral stability curve is drastically influenced by Cr and Bo for α typically less than 2, yet the spatial shapes of the disturbance variables remain unchanged at a given α. For both limiting cases, the normalized eigenvectors of $\chi_k(x_3)$ are identical for all k,

[3] If the kth stratifying agency is temperature, the kth transport equation is the energy equation and Nu_k is defined as $Nu_k = h_k d/\rho c_p \mathscr{D}_k$.

however, in the following section, we show that neutral stability boundaries in the presence of deformation are influenced by $\mathscr{D}_{\mathrm{k}}$.

3.2. Stationary solution and limiting cases

Substituting the spatial shapes, eqns (18) and (19), into the tangential stress equation, eqn (15), yields an exact solution for stationary stability of a multicomponent system. The use of general disturbance flux conditions allows for finite Nu_k values at both boundaries and also eliminates the need for separate solutions for different limiting cases [9–14, 18–22] which becomes impractical as the number of stratifying agencies, N, increases. A tedious solution process remains unavoidable, particularly with the incorporation of mixed flux conditions at both boundaries. However, after substantial manipulations, a surprisingly concise solution emerges as

$$8\alpha\left(\alpha-\frac{1}{2}\sinh 2\alpha\right)+\sum_{k=1}^{N} Ma_k \frac{(\sinh^2\alpha\tanh\alpha-\alpha^3)Nu_k^{(l)}+\alpha((\alpha^2+\sinh^2\alpha)-(2+\alpha^2)\alpha\tanh\alpha)+\dfrac{8Cr\mathscr{D}_k\alpha^5(\alpha\tanh\alpha+Nu_k^{(l)})}{(Bo+\alpha^2)}}{(\alpha^2+Nu_k^{(l)}Nu_k^{(u)})\tanh\alpha+\alpha(Nu_k^{(u)}+Nu_k^{(l)})}=0 \tag{21}$$

In this form it is easy to see that the singly diffusive solutions of [9, 10 and 12], the doubly diffusive solutions of [18, 21] and previously unreported solutions for three or more stratifying agencies are obtained for $N=1$, $N=2$ and $N \geqslant 3$, respectively.

We again refer to the two limiting cases presented in Table 1, with the understanding that other significant parameter limits could also be explored. In both limits, $Nu_k^{(l)} \to \infty$ and $Nu_k^{(l)} \to 0$, the resulting multicomponent solutions can be recast as effective single component solutions. Equation (22) corresponds to $Nu_k^{(l)} \to \infty$ (for all k) and eqn (23) corresponds to $Nu_k^{(l)} \to 0$, (for all k).

$$Ma_\Sigma=\frac{8\alpha^2\left(\alpha-\dfrac{1}{2}\sinh 2\alpha\right)}{\alpha^3-\sinh^2\alpha\tanh\alpha-\dfrac{8\alpha^5 Cr\tilde{\mathscr{D}}}{\alpha^2+Bo}} \tag{22}$$

$$Ma_\Sigma=\frac{8\alpha^2\left(\alpha-\dfrac{1}{2}\sinh 2\alpha\right)}{\alpha^3+2\alpha-\alpha^2\coth\alpha-\dfrac{1}{2}\sinh 2\alpha-\dfrac{8\alpha^5 Cr\tilde{\mathscr{D}}}{\alpha^2+Bo}} \tag{23}$$

where Ma_Σ denotes the summation of the Ma_k, and $\tilde{\mathscr{D}}$ is a Marangoni number weighted average of the diffusivity ratios, $\mathscr{D}_k$:

$$Ma_\Sigma=\sum_{k=1}^{N} Ma_k, \quad \text{and} \quad \tilde{\mathscr{D}}=\frac{\sum_{k=1}^{N} Ma_k\mathscr{D}_k}{Ma_\Sigma}$$

The above formulations demonstrate the equivalence between the multicomponent solution for arbitrary N-stratifying agencies and the single component problem. The single component formulations, eqns (22) and (23), are insightful, although it is typically more convenient to compute neutral stability values of Ma_j ($j \neq k$) directly from eqn (21). They also play a central part in our examination of frontier point behavior in multicomponent systems.

For a flat interface, $Cr=0$, the $\tilde{\mathscr{D}}$ term is eliminated, and it is apparent that the Ma_k are additive with their sum, Ma_Σ, fixed for given α. In these special cases, we note that similar conclusions also follow for the flat interface from inspection of the normal mode equations for $\lambda=0$. Consistent with the single component layer, multicomponent critical values, (α_c, $(Ma_\Sigma)_c$), are (1.993, 79.604) and (0,48) for the respective Table 1 cases. This is a direct generalization of the conclusion reached by McTaggart [18] for the double diffusive layer with a flat interface. In their double diffusive analysis, Char and Chiang [22] report oscillatory neutral stability results for $\mathscr{D}_2=0.04$ while stationary stability results are reported for $\mathscr{D}_2=1$. Including the effect of surface deformation, they note an additive or direct reinforcement nature of Ma_1 and Ma_2 in the case of stationary onset. Their observation is consistent with our results for $\mathscr{D}_2=1$, but it fails to hold when $\mathscr{D}_2 \neq 1$. For $\mathscr{D}_2 \neq 1$, the relationship between Ma_1 and Ma_2 is modified by the presence of $\mathscr{D}_2$ in the deflection (Cr) term of eqns (21) and (22) for stationary onset. In a multicomponent layer, $N \geqslant 2$, we find that Char and Chiang's direct reinforcement of Ma_k similarly holds when $\mathscr{D}_{\mathrm{k}}=1$ (for all k). However, in the presence of surface deflection, $\tilde{\mathscr{D}}$ is no longer negligible, as variations among $\mathscr{D}_k$ can have a profound effect on neutral (stationary) stability, especially for infinitesimal wavenumber.

Although the neutral stability solutions, eqns (22) and (23), are of indeterminant forms at $\alpha=0$, the limit $\alpha \to 0$ merits examination because onset of convection often occurs at an infinitesimal wavenumber for various boundary flux and surface deformation parameter values.

Characterization of the stability behavior in this limit is also required for investigating frontier point boundaries. Successive application of L'Hospital's rule to eqns (22) and (23) yield the following stationary stability relations for a multicomponent layer in the limit $\alpha \to 0$.

$$\frac{2}{3}\frac{Bo}{Cr} = Ma_\Sigma \tilde{\mathscr{D}} \quad (\text{for } Nu_k^{(l)} \to \infty, \text{ all } k) \tag{24}$$

$$\frac{2}{3}\frac{Bo}{Cr} = \frac{\tilde{\mathscr{D}}}{1-\dfrac{Ma_\Sigma}{48}} \quad (\text{for } Nu_k^{(l)} \to 0, \text{ all } k) \tag{25}$$

For a singly diffusive layer, eqn (24) agrees with the small wavenumber results of [11, 13, 24], $Ma_1 = 2/3\ Bo/Cr$, and further confirms the numerical results of [14, 22]. Extending the analysis to the other flux limit, $Nu_k^{(l)} \to 0$, we find that onset of convection always occurs in the limit $\alpha \to 0$ as for a flat interface and that eqn (25) yields the multicomponent exact solution for the critical value(s) $(Ma_k)_c$. For example, Ma_c is given by $Ma_1 = 48(1+72\ Cr/Bo)^{-1}$ for a singly diffusive layer. In both cases, Ma_1 is a function of a single parameter, the ratio (Cr/Bo) in the $\alpha \to 0$ limit. For a permeable (conductive) surface at $x_3 = 0$, Ma_1 takes on values, $0 < Ma_1 < \infty$, over the range $0 < Bo/Cr < \infty$ while Ma_1 is bounded in the interval $0 < Ma_1 < 48$ for an impermeable (insulated) lower surface for the previous Bo/Cr range.

Using the single component problem for validation, Char and Chiang [22] confirmed that their small wavenumber neutral stability results approached the analytical results reported in [11, 25] for the limit $\alpha \to 0$. Their double diffusive stationary results for nonzero Ma_2 (-100 and 100) also agree with the exact solution, eqn (24), for the limit $\alpha \to 0$, although the relationship, $Ma_{1c}+Ma_{2c} = Ma_c$, holds only for $\mathscr{D}_2 = 1$, as discussed for the finite wavenumber case. We find from eqn (24) that the exact double diffusive solution for Ma_1 in the limit $\alpha \to 0$ is expressed as:

$$Ma_1 = \frac{2}{3}\frac{Bo}{Ca} - \mathscr{D}_2 Ma_2$$

where the stationary values of Ma_1 are translated up or down by the product $(\mathscr{D}_2 Ma_2)$. When stationary onset occurs at finite wavenumber, e.g. $\alpha \approx 2$, the deviation from ignoring the $\mathscr{D}_k$ dependence is often small. When onset occurs at infinitesimal wavenumber, large errors in Ma_1 are likely for nonzero Ma_2. For $Nu_k^{(l)} \to 0$ an exact relation for Ma_1 (or other Ma_k) involving N-stratifying agencies is similarly obtained from eqn (25).

3.3. Frontier points

For certain parameter value sets, onset of convection can occur simultaneously at two different modes. This set of parameters where two spatial modes can coexist during onset has more recently been referred to as a frontier point [14, 22]. Dynamics in the region of a frontier point is anticipated to be complex. For example, Proctor and Jones [28] observed interesting dynamical behavior when two modes compete in destabilizing a two-fluid system while similar nonlinear analyses are identified in [14]. A practical consequence of identifying frontier points or frontier boundaries is that a quantitative criterion is then established for determining which of the competing modes occurs at convective onset for a given set of parameter values. In the ensuing analysis this parameter set is (α, Ma_k, $\mathscr{D}_k$, Cr, Bo). The component flux conditions given in Table 1 are again applied. Because stationary onset always occurs in the limit $\alpha \to 0$ for $Nu_k^{(l)} \to 0$ this case need not be considered any further. The case of $Nu_k^{(u)} \to 0$ and $Nu_k^{(l)} \to \infty$, for all k, has received recent attention [14, 22], and a single frontier point (Bo, Cr) has been identified in these studies.

The existence of frontier points is confirmed by the neutral stability curves for four different (Bo, $\tilde{\mathscr{D}}Cr$) values shown in (α, Ma_Σ) space in Fig. 1. For (Bo, $\tilde{\mathscr{D}}Cr$) values of (0.05, 0.0006) and (0.05, 0.0003) convective onset occurs at infinitesimal and finite wavenumber, $\alpha \approx 2$, respectively. Convective onset occurs simultaneously at two different spatial modes for the two remaining curves, i.e. frontier points exist at (Bo, $\tilde{\mathscr{D}}Cr$) values of (0.05, 0.0004212) and (0.5, 0.004456). Decreasing $\tilde{\mathscr{D}}Cr$ for constant Bo leads to stabilization at small wavenumbers which is consistent with the view [11, 14, 22] that increasing Bo for a given Cr is stabilizing. In Fig. 1, we find that $(\tilde{\mathscr{D}}Cr)_{\mathrm{fp}}$ increases with increasing Bo, while $Ma_{\Sigma\mathrm{fp}}$ and α_{fp} decrease. The neutral stability curves flatten considerably for wavenumbers less than α_{fp}, as the frontier parameter values (Bo_{fp}, $\tilde{\mathscr{D}}Cr_{\mathrm{fp}}$) are increased. While the parameters, Ma_Σ and $\tilde{\mathscr{D}}$, allow for consideration of a multicomponent fluid layer, they are also applicable to the case of a singly diffusive layer, $N = 1$, by treating Ma_Σ as Ma_1 and setting $\tilde{\mathscr{D}} = 1$.

As in the case of stationary stability boundaries, $\mathscr{D}_2$ has no effect on frontier point behavior for a flat interface, $Cr = 0$, however this is not true when deformation is included. In their numerical analysis of a double diffusive layer with deformation, Char and Chiang [22] examined frontier point behavior at a Bo value of 0.1 and $\mathscr{D}_2 = 1$. Extending this work, we explore this behavior for $\mathscr{D}_2$ values more typically encountered in thermosolutal and double diffusive systems using the exact solution, eqn (22). Frontier point curves for Ma_2 values for 100 and -100 are shown in Figs 2 and 3, respectively. Variations of $\mathscr{D}_2$ dramatically affect the value of Cr_{fp}, while $Ma_{1\mathrm{fp}}$ and α_{fp} are independent of its value. The local maximum value of Ma_1 between the two critical modes decreases (increases) for positive (negative) Ma_2 and $\mathscr{D}_2$ decreases. The flattening effect of $\mathscr{D}_2$ is pronounced for positive Ma_2. For values of $\mathscr{D}_2$ typical of thermosolutal systems, $\mathscr{D}_2 < 10^{-2}$, the minima and local maximum becomes visibly indistinguishable in Fig. 2. For negative Ma_2,

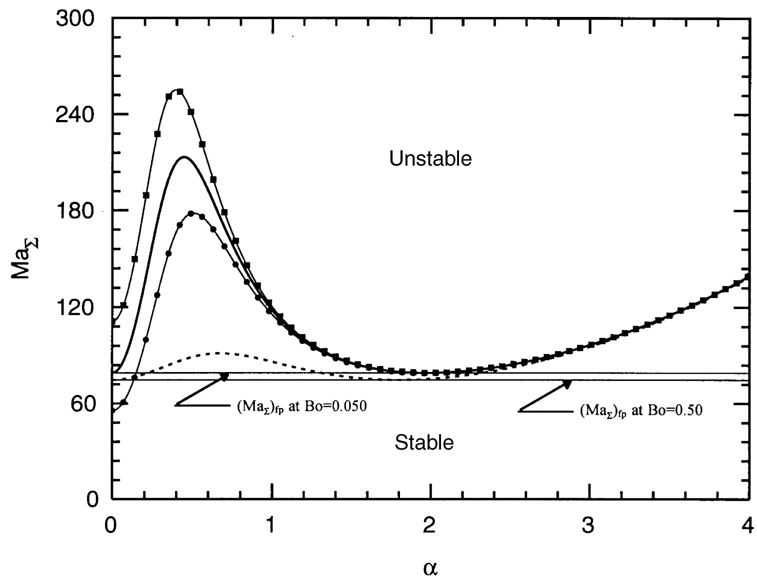

Fig. 1. Stationary stability boundaries for different values of Bo and $(\tilde{\mathscr{D}}Cr_{fp})$. Two curves shown are taken at frontier points associated with Bo values of 0.05 and 0.50: —— $Bo = 0.05$, $(\tilde{\mathscr{D}}Cr_{fp}) = 4.214\times10^{-4}$; · · · · · · $Bo = 0.05$, $(\tilde{\mathscr{D}}Cr_{fp}) = 6.000\times10^{-4}$; —■— $Bo = 0.05$, $(\tilde{\mathscr{D}}Cr_{fp}) = 3.000\times10^{-4}$; —●— $Bo = 0.50$, $(\tilde{\mathscr{D}}Cr_{fp}) = 4.456\times10^{-3}$.

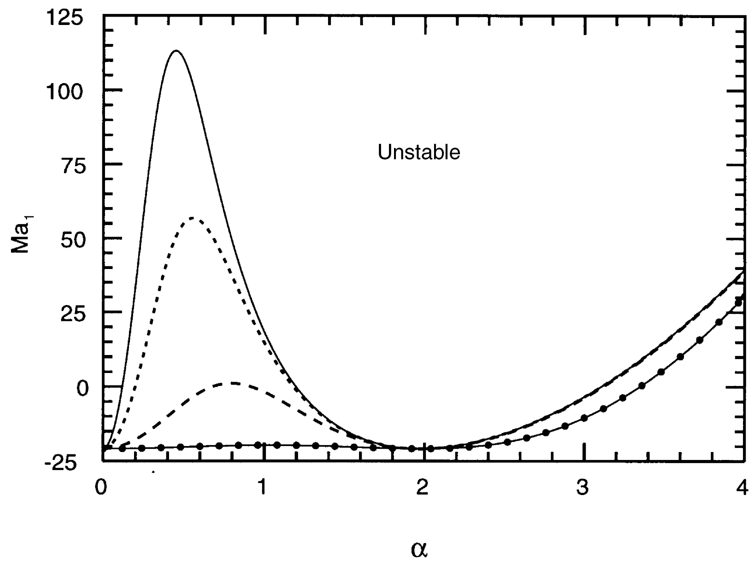

Fig. 2. The influence of $\mathscr{D}_2$ on frontier point stationary stability boundaries for $Ma_2 = 100$, $Bo = 0.05$, $\alpha_{fp} = 1.975$: —— $\mathscr{D}_2 = 1.00$, $Cr_{fp} = 4.212\times10^{-4}$; - - - - - - $\mathscr{D}_2 = 0.50$, $Cr_{fp} = 1.144\times10^{-3}$; — — — $\mathscr{D}_2 = 0.25$, $Cr_{fp} = 8.045\times10^{-3}$; —●— $\mathscr{D}_2 = 0.23$, $Cr_{fp} = 2.321\times10^{-1}$.

Fig. 3 reveals that the local maximum is bounded for $0 < \mathscr{D}_2 < 1$.

In general, values of Cr_{fp} are strongly influenced by both $\mathscr{D}_2$ and Ma_2 for the double diffusive problem. Comparing Figs 2 and 3, we find that the value of Cr_{fp} increases with decreasing $\mathscr{D}_2$ for positive Ma_2 and decreases with negative Ma_2 when Bo is constant. In Fig. 2, stationary onset occurs at $\alpha = 1.975$ in a double diffusive layer with $\mathscr{D}_2 < 0.5$ and Cr of 0.001, and in the long wave length limit, $\alpha \to 0$, for $\mathscr{D}_2 = 1$. In a double diffusive layer, with $\mathscr{D}_2$, Bo and Cr values of 0.05, 0.5 and 0.001, respectively, stationary onset occurs at the finite wavenumber,

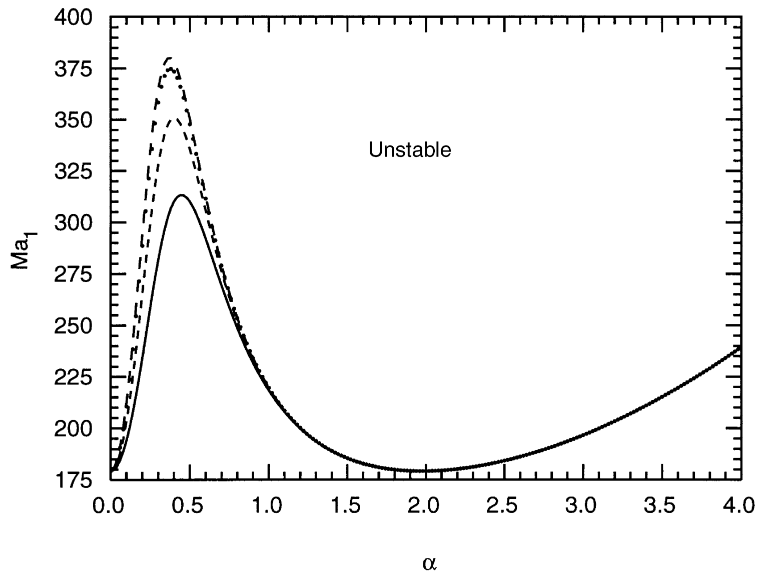

Fig. 3. Influence of $\mathscr{D}_2$ on frontier point stationary stability boundaries for $Ma_2 = -100$, $Bo = 0.05$, $\alpha_{fp} = 1.975$: —— $\mathscr{D}_2 = 1$, $Cr_{fp} = 4.212\times10^{-4}$; ------ $\mathscr{D}_2 = 0.5$, $Cr_{fp} = 2.581\times10^{-3}$; $\cdots\cdots$ $\mathscr{D}_2 = 0.1$, $Cr_{fp} = 1.971\times10^{-3}$; — — — $\mathscr{D}_2 = 0.01,\ 0.001,\ 0$, $Cr_{fp} = 1.861\times10^{-4}$.

$\alpha_c = 1.975$ when Ma_2 is positive, $Ma_2 = 100$. However, for negative Ma_2 ($Ma_2 = -100$ in Fig. 3), Cr exceeds Cr_{fp} and onset occurs in the long wave length limit, $\alpha \to 0$.

The multicomponent problem was recast as a single component problem leading to stationary stability solutions, eqns (22–25) with the aid of Ma_Σ and $\tilde{\mathscr{D}}$. An interesting characteristic of this reformulation is that it allows frontier boundaries for an arbitrary number of stratifying agencies, and varying values of $\mathscr{D}_k$ and Ma_k to be described by a single curve. This is demonstrated in Fig. 4 where the frontier boundary spans over six orders of magnitude in (Bo, $\tilde{\mathscr{D}}Cr$) space. The boundary directly applies to the single component system by setting $\tilde{\mathscr{D}}$ to 1 and Ma_Σ to Ma_1. Along the frontier boundary, two spatial modes compete to destabilize the fluid layer. To the left and above the frontier boundary in Fig. 4, onset of instability is associated with the infinitesimal wavenumber mode, $\alpha \to 0$, while to the right and below the boundaries, onset of convection is associated with finite wavenumber modes. The frontier boundary for $\tilde{\mathscr{D}} > 0$ is described quite well by the fitted equation, $\tilde{\mathscr{D}}Cr/Bo^{1.01} = 0.00893$, for the range of Bo examined, $5\times10^{-7} \leqslant Bo \leqslant 1$. Thus we find for $\tilde{\mathscr{D}}Cr/Bo^{1.01} > 0.00893$ stationary onset is characterized by a large global circulation cell, $\alpha \to 0$, while finite sized convection cells occur when the inequality is reversed.

While $\tilde{\mathscr{D}}$ can take on negative values when

$$Ma_\Sigma < \sum_{k=2}^{N} (1-\mathscr{D}_k)Ma_k,$$

our results suggest that $Ma_\Sigma\tilde{\mathscr{D}}$ must be positive for a frontier point to exist. Subject to the condition that $Ma_\Sigma|_{\alpha\to0}$ is a local minimum, $Ma_\Sigma\tilde{\mathscr{D}} > 0$ is necessary for the existence of a frontier point, as described in the Appendix. The extremum boundary given by eqn (A.7) in the Appendix, is shown in Fig. 4 insert as a dotted line. Above and to the left of extremum boundary curve (dotted line), $Ma_{\Sigma|_{\alpha\to0}}$ is a minimum; while below and to the right of the boundary curve, $Ma_{\Sigma|_{\alpha\to0}}$ is a local maximum. As would be expected, the frontier boundary in Fig. 4 lies above the extremum boundary curve guaranteeing that one local minima occurs in the long wavelength limit, $\alpha \to 0$. The extremum boundary curve approaches the frontier boundary with increasing Bo over the range of Bo investigated, $10^{-7} \leqslant Bo \leqslant 1$.

Selected frontier point values shown in Figs 4 and 5 are given in Table 2. For the single Bo value of 0.1, Perez-Garcia and Carneiro [14] computed frontier points for the singly diffusive layer varying the relative importance of buoyancy and surface tension variation. They found that the minimum Cr value, 8.47×10^{-3} at which a frontier point existed occurred in the absence of buoyancy. This frontier point which is identified in Fig. 4 was similarly obtained in the double diffusive fluid layer for $\mathscr{D}_2 = 1$ [22]. Inspection of eqn (22) and Fig. 4 reveal that the stationary stability behavior of the singly diffusive system [14] and doubly diffusive system [22] are equivalent when $\mathscr{D}_2 = 1$.

The allowable values of Ma_k for which two spatial modes coexist during stationary onset of convection are also restricted by the possibility of oscillatory instability. While our analysis is confined to stationary stability,

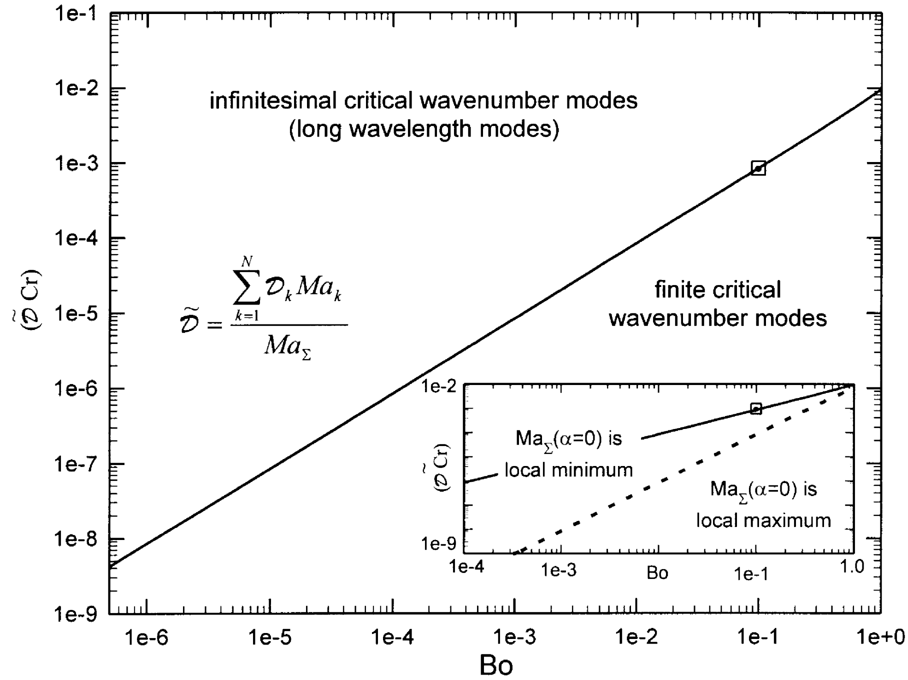

Fig. 4. Frontier point boundaries in (Bo, $\tilde{\mathscr{D}}Cr$) space: ▣ represents frontier point identified in [14, 22]. Curve fit: $\tilde{\mathscr{D}}Cr = 8.93 \times 10^{-3} Bo^{1.01}$; $R = 0.99994$. The dotted line in the insert is the extremum boundary for Ma_Σ ($\alpha = 0$). Above the dotted line, Ma_Σ ($\alpha = 0$) is a local maximum, below this line it is a local minimum: —— frontier boundary; - - - - - - extremum boundary for Ma_Σ ($\alpha = 0$).

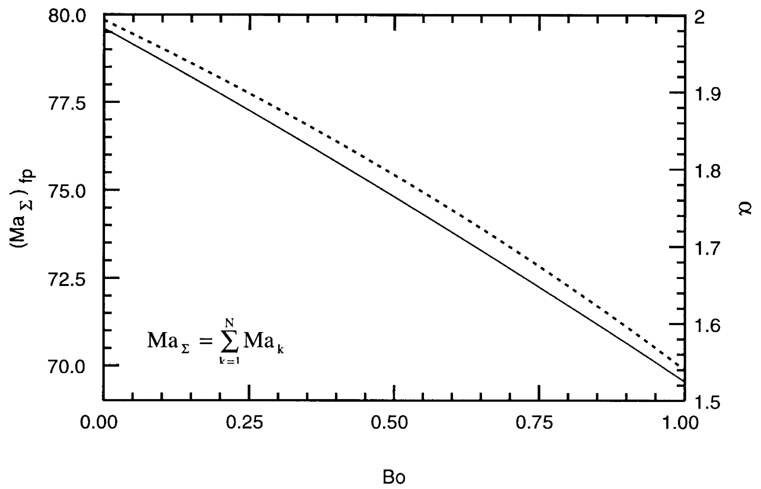

Fig. 5. Critical finite wavenumber, α_{fp}, and Ma_Σ values associated with frontier boundaries: —— Ma_Σ - - - - - - α_{fp}.

oscillatory convective onset is possible when one or more of the N-components with $\mathscr{D}_k < 1$, is stabilizing, i.e. $Ma_k < 0$. Three types of frontier points, characterized by two coexisting modes that have been identified in the extensive analyses by Perez-Garcia and Carneiro [14] and Char and Chiang [22] are: both stationary modes, both oscillatory modes, or one stationary/one oscillatory mode. Our study has focused on the coexistence of stationary modes for broad ranges of Bo, Ma_k and $\mathscr{D}_k$ values, however, the influences of these parameters on the other two types of frontier points remain largely unexplored for the multicomponent layer.

Table 2
Selected frontier point parameter values corresponding to Figs 4 and 5

Bo	$(\tilde{\mathscr{D}}Cr)_{\mathrm{fp}}$	$(Ma_{\Sigma})_{\mathrm{fp}}$	α_{fp}
0.0001	$8.375\ 10^{-7}$	79.606	1.993
0.001	$8.375\ 10^{-6}$	79.598	1.993
0.01	$8.384\ 10^{-5}$	79.514	1.989
0.05	$4.212\ 10^{-4}$	79.144	1.975
0.1	$8.473\ 10^{-4}$	78.677	1.956
1.0	$9.586\ 10^{-3}$	69.544	1.540

Table 3
Bo and *Cr* values for common liquids

	Pr	Bo	Cr	$\mathscr{D}_2$
Water	5.83	0.0343	3.53E-06	—
Mercury	0.0248	0.0703	2.92E-05	—
Glycerin	6780	0.0490	0.00237	—
Silicone oil	105	0.1141	8.85E-05	—
Water–ethanol[1]	7.7	0.04301	6.47E-06	0.008

($d = 0.5$mm, $g = 9.81$ m s^{-2}) property values chosen at approximately 300 K.
[1] Water–ethanol mixture 4% ethanol by weight.

Bo and *Cr* values of common fluids for a layer depth of 0.5 mm and in a 1-g gravity environment are given in Table 3. For a singly diffusive layer, values of the first four fluids are in agreement with those reported in [11]. Examination of Figs 4 and 5, reveals that onset will occur at finite wavenumbers for water, mercury, and Silicone oil, while onset occurs at infinitesimal wavenumber for Glycerin. In a reduced gravity environment of $10^{-5}\,g$, *Bo* decreases by five orders of magnitude, and Fig. 4 indicates that onset occurs at infinitesimal wavenumber for all Table 3 fluids. Evaluation of a frontier point behavior for the water-ethanol thermosolutal system proceeds as follows. First $(\tilde{\mathscr{D}}Cr)_{\mathrm{fp}}$ and $(Ma_{\Sigma})_{\mathrm{fp}}$ values of 3.62×10^{-4} and 79.2 corresponding to $Bo = 0.0430$ are obtained from Figs 4 and 5, respectively, or computed from eqns (22) and (24). The $\tilde{\mathscr{D}}$ values, 0.373, 0.00310 and -0.252 are computed using the three Ma_2 values, 50, 79.6 and 100 given in Fig. 6. As indicated in the Appendix, the negative $Ma_{\Sigma}\tilde{\mathscr{D}}$ value immediately rules out a frontier point for $Ma_2 = 100$. Onset occurs at a finite wavenumber as observed in Fig. 6 for the stability curve associated with $Ma_2 = 100$. The above condition, requires that $Ma_2 < 79.85$ for a frontier point to occur. For the remaining two Ma_2 values, Cr_{fp} is greater than the Table 3 *Cr* value, therefore, onset occurs at finite wavenumber. The corresponding neutral stability curves at Cr_{fp} and Table 3 Cr values are also shown in Fig. 6. Re-evaluating for 10^{-5} g, leads to convective onset at an infinitesimal wavenumber similar to the singly diffusive systems.

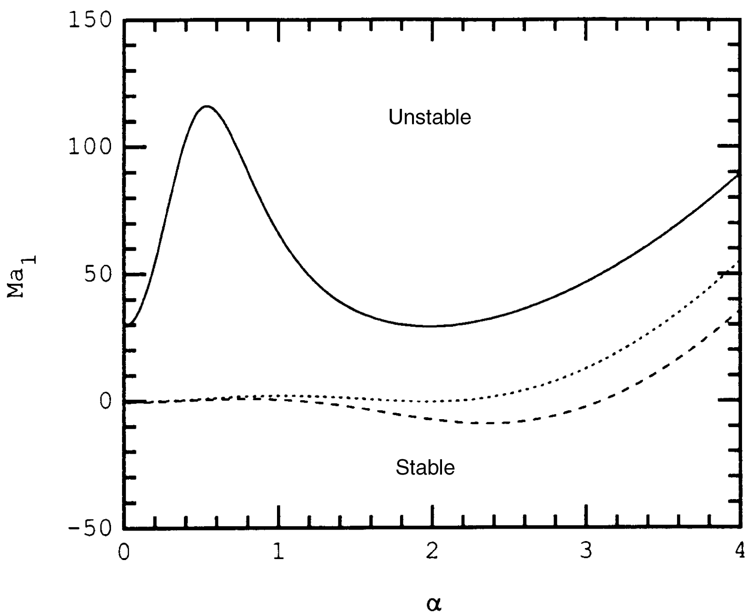

Fig. 6. Neutral stability curves for double diffusive (water–ethanol) system, $\tilde{\mathscr{D}}_2 = 0.008$, $Bo = 0.0430$:. —— $Ma_2 = 50$, $\tilde{\mathscr{D}} = 0.374$; $\cdots\cdots$ $Ma_2 = 79.6$, $\tilde{\mathscr{D}} = 0.003$; - - - - - - $Ma_2 = 100$, $\tilde{\mathscr{D}} = -0.252$.

4. Conclusions

Traditional analyses have been used to examine the stationary onset of convection in a multicomponent fluid layer due to surface tension variation along a free surface. Deformation and gravity effects at the free surface have been treated, and mixed flux conditions have been applied to the stratifying agency transport equations at both boundaries. An exact solution for neutral stability owing to an exchange of stabilities, and valid for N-stratifying agencies, has been obtained. In addition, the solution was evaluated in the limit $\alpha \to 0$. For two limiting sets of boundary conditions examined, the spatial shapes of velocity and the stratifying agencies are invariant with all parameters except wavenumber. The spatial shapes then remain unchanged at stationary onset in a multicomponent system for any combination of Ma_k under these circumstances.

The loci of points along which two modes can occur simultaneously has been determined over a range of Bo, $10^{-7} \leqslant Bo \leqslant 1$ for the limit flux conditions $(Nu_k^{(l)}, Nu_k^{(u)}) \to (\infty, 0)$. Frontier points in ($Bo$, Cr) space are found to be functions of Ma_k and $\mathscr{D}_k$ but can be presented as a single frontier boundary curve in (Bo, $\tilde{\mathscr{D}}Cr$) space that accounts for different values of Ma_k, $\mathscr{D}_k$ and Bo of a multicomponent system with arbitrary N-stratifying agencies. The frontier boundary was represented quite well by the empirical relation, $(\tilde{\mathscr{D}}Cr)_{\mathrm{fp}} = (Bo_{\mathrm{fp}})^{1.01}$ 0.00893 for range of Bo specified above. For $Bo > 0$, the existence of a frontier point requires that $(Ma_\Sigma \tilde{\mathscr{D}})$ be a positive value.

Acknowledgement

This work was performed as part of NASA's Microgravity Fund Physics Program and supported by NASA's Microgravity Sciences Division.

Appendix

Assumptions and conditions related to the existence of frontier points

Equation (22), which is the multicomponent stationary neutral stability solution for flux conditions, $(Nu_k^{(l)}, (Nu_k^{(u)}) \to (\infty, 0)$, can be written in the following form:

$$\frac{8\alpha^2\left(\frac{1}{2}\sinh 2\alpha - \alpha\right)}{\sinh^2\alpha\tanh\alpha - \alpha^3 + \dfrac{8\alpha^5 Cr}{\alpha^2 + Bo}} = \sum_{k=1}^{N} Ma_k Y_k \tag{A.1}$$

where:

$$Y_k = \frac{\sinh^2\alpha\tanh\alpha - \alpha^3 + \dfrac{8\alpha^5 Cr\mathscr{D}_k}{\alpha^2 + Bo}}{\sinh^2\alpha\tanh\alpha - \alpha^3 + \dfrac{8\alpha^5 Cr}{\alpha^2 + Bo}} \tag{A.2}$$

In Section 2 the stratifying agency with the largest $\mathscr{Q}$ was declared the $k = 1$ component. Additionally, $\mathscr{Q}_k > 0$ for all k, therefore the diffusivity ratio, $\mathscr{D}_k$, is bounded within the range $0 < \mathscr{D}_k \leqslant 1$.[4] $Bo \geqslant 0$ to preclude the Rayleigh–Taylor instability [11]. Takashima [13, 14] has theoretically examined the case of $Bo < 0$ for a single component layer, however, such basic states have not been observed experimentally, and may not be physically realizable as he [14] notes as well. Given these constraints on Bo and $\mathscr{D}_k$, the left-hand side of eqn (A.1) is always positive, therefore,

$$\sum_{k=1}^{N} Ma_k Y_k \geqslant 0$$

and eqn (A.2) requires $0 \leqslant Y_k \leqslant 1$. This leads to the following inequalities,

$$\sum_{k=1}^{N} \left|Ma_k\right| \geqslant \sum_{k=1}^{N} \left|Ma_k Y_k\right|$$

and

$$\sum_{k=1}^{N} \left|Ma_k\right| \geqslant \sum_{k=1}^{N} \left|Ma_k \mathscr{D}_k\right|$$

which are useful in establishing property and parameter bounds, or estimating parameter values, such as given Ma_k, $\mathscr{D}_k$ or $Ma_k\mathscr{D}_k$.

In terms of Ma_Σ and $\tilde{\mathscr{D}}$ eqn (A.1) gives:

$$\frac{8\alpha^2\left(\frac{1}{2}\sinh 2\alpha - \alpha\right)}{\sinh^2\alpha\tanh\alpha - \alpha^3 + \dfrac{8\alpha^5 Cr}{\alpha^2 + Bo}} = Ma_\Sigma(k_1 + k_2\tilde{\mathscr{D}}) \tag{A.3}$$

where

$$k_1 = \left(1 + \frac{8\alpha^5 Cr}{(\alpha^2 + Bo)(\sinh^2\alpha\tanh\alpha - \alpha^3)}\right)^{-1} \tag{A.4}$$

$$k_2 = \left(\frac{(\alpha^2 + Bo)(\sinh^2\alpha\tanh\alpha - \alpha^3)}{8\alpha^5 Cr} + 1\right)^{-1} \tag{A.5}$$

Again noting the earlier constraints on Bo and $\mathscr{D}_k$, eqn (A.3) requires that $Ma_\Sigma(k_1 + k_2\tilde{\mathscr{D}}) \geqslant 0$, while k_1 and k_2 are bounded as $0 \leqslant k_1, k_2 \leqslant 1$. Consequently, if $\tilde{\mathscr{D}} \geqslant 0$, it follows that $Ma_\Sigma > 0$. Although $\tilde{\mathscr{D}}$ can take on negative

[4] This would not apply when cross-diffusion, such as the Soret or Dufour effect, is important, since negative cross-diffusive coefficients are possible [8, 24, 26, 27].

values, our study of frontier boundaries is confined to, $\tilde{\mathscr{D}} > 0$, thus also requiring $Ma_\Sigma > 0$.

Subject to the constraint that one minimum is located in the long wavelength limit, $\alpha \to 0$, then the following condition obtained from eqn (24) is necessary for the existence of a frontier point:

$$Ma_\Sigma \tilde{\mathscr{D}} = \sum_{k=1}^{N} Ma_k \mathscr{D}_k > 0.$$

Both Cr and Bo are taken to be positive quantities. In the long wavelength limit, $\alpha \to 0$, $\mathrm{d}Ma/\mathrm{d}\alpha|_{\alpha\to 0} = 0$, demonstrating that this limit is a local extremum for finite values of Cr and Bo. The nature of the extremum; maximum or minimum, is parameter dependent and is determined from the sign of eqn (A.6).

$$\mathrm{d}^2(Ma_\Sigma)/\mathrm{d}\alpha^2|_{\alpha\to 0} = \frac{120\tilde{\mathscr{D}}Cr + 24Bo\tilde{\mathscr{D}}Cr - Bo^2}{90(\tilde{\mathscr{D}}Cr)^2} \quad \text{(A.6)}$$

The long wavelength limit, $\alpha \to 0$, is a local minimum when $120\tilde{\mathscr{D}}Cr + 24Bo(\tilde{\mathscr{D}}Cr) - Bo^2 > 0$ and a local maximum when $120\tilde{\mathscr{D}}Cr + 24Bo(\tilde{\mathscr{D}}Cr) - Bo^2 < 0$. Accordingly, the extremum boundary, separating these two extremum conditions is given by eqn (A.7) and shown in Fig. 4 insert.

$$\tilde{\mathscr{D}}Cr = \frac{Bo^2}{120 + 24Bo} \quad \text{(A.7)}$$

Equation (A.7), which is determined directly from eqn (22), is similar to the expression Takashima [12] obtained by expanding his single component solution in powers of α.

References

[1] J.S. Turner, Multicomponent convection, Ann. Rev. Fluid Mech. 17 (1985) 11–44.

[2] J.S. Turner, Double-diffusive phenomena, Ann. Rev. Fluid Mech. 6 (1974) 37–56.

[3] M.E. Stern, The salt-fountain and thermohaline convection, Tullus 12 (1960) 599–611.

[4] R.W. Griffiths, The influence of a third diffusing component upon the onset of convection, J. Fluid Mech. 92 (1979) 659–670.

[5] J.K. Platten, J.C. Legros, Convection in Liquids, Springer-Verlag, New York, 1984.

[6] Torrones and Pearlstein, The onset of convection in a multicomponent fluid layer, Phys. Fluids A 1 (5) (1989) 845–853.

[7] Lord Rayleigh, On convection currents in a horizontal layer of fluid when the higher temperature is on the under side, Phil. Mag. 32 (1916) 529–546.

[8] D.T.J. Hurle, E.J. Jakeman, Soret-driven thermosolutal convection, J. Fluid Mech. 47 (1971) 667–687.

[9] J.R.A. Pearson, On convection cells induced by surface tension, J. Fluid Mech, 4 (1958) 489–500.

[10] L.E. Scriven, C.V. Sternling, On cellular convection driven by surface-tension gradients: effects of mean surface tension and surface viscosity, J. Fluid Mech. 19 (1964) 321–340.

[11] K.A. Smith, On convective instability induced by surface-tension gradients, J. Fluid Mech. 24 (2) (1966) 401–414.

[12] M. Takashima, Surface tension driven instability in a horizontal liquid layer with a deformable free surface—I: stationary convection, J. Phys. Soc. Japan 50 (8) (1981) 2745–2750.

[13] M. Takashima, Surface tension driven instability in a horizontal liquid layer with a deformable free surface—II: overstability, J. Phys. Soc. Japan 50 (8) (1981) 2751–2756.

[14] C. Perez-Garcia, G. Carneiro, Linear stability analysis of Benard–Marangoni convection in fluids with a deformable free surface, Phys. Fluids A 3 (2) (1991) 292–298.

[15] E.L. Koschmieder, Benard Cells and Taylor Vortices, Cambridge University Press, 1993.

[16] S. Davis, Thermocapillary instabilities, Ann. Rev. Fluid Mech. 19 (1987) 403–435.

[17] J.C. Legros, O. Dupont, P. Queeckers, S. Van Vaerenbergh, D. Schwabe, Thermohydrodynamic instabilities and capillary flows, in: J.N. Coster, R.L. Sani (Eds.), Low-Gravity Fluid Dynamics and Transport Phenomenon, Progress in Astronautics and Aeronautics, 1990.

[18] C.L. McTaggart, Convection driven by concentration and temperature dependent surface tension, J. Fluid Mech. 134 (1983) 301–310.

[19] C.F. Chen, T.F. Su, Effect of surface tension on the onset of convection in a double-diffusive layer, Phys. Fluids 4 (11) (1992) 2360–2367.

[20] J. Tanny, C.C. Chen, C.F. Chen, Effects of interaction between Marangoni and double-diffusive instabilities, J. Fluid Mech. 303 (1995) 1–21.

[21] F.E. McCaughan, H. Bedir, Marangoni convection with a deformable free surface, AMD-Vol. 154/FED-Vol. 142, Fluid Mechanics Phenomena In Microgravity ASME, 1992.

[22] M. Char, K. Chiang, Effect of interfacial deformation on the onset of convective instability in a doubly diffusive fluid layer, Int. J. Heat Mass Transfer 39 (2) (1996) 407–419.

[23] S. Chandrasekhar, Hydrodynamic and Hydromagnetic Stability, Dover Publications, 1981.

[24] J.R.L. Skarda, D. Jacqmin, F.E. McCaughan, Exact and approximate solution to the double-diffusive Marangoni–Benard problem with cross-diffusive, J. Fluid Mech. 366 (1998) 109–133.

[25] S. Davis, Rupture of thin films, in: R.E. Meyer (Ed.), Waves on Fluid Interfaces, 1983, pp. 291–302.

[26] G. Zimmermann, U. Muller, S.H. Davis, Benard convection in binary mixtures with Soret effects and solidification, J. Fluid Mech. 238 (1992) 657–682.

[27] C.F. Chen, C.C. Chen, Effect of surface tension on the stability of a binary fluid layer under reduced gravity, Phys. Fluids 6 (1994) 1482–1490.

[28] M.R.E. Proctor, C.A. Jones, The interaction of two spatially resonant patterns in thermal convection—part 1: exact 1 : 2 resonance, J. Fluid Mech. 188 (1988) 301–335.